European Journal of Cell Biology 99 (2020) 151096

Contents lists available at ScienceDirect

European Journal of Cell Biology

journal homepage: www.elsevier.com/locate/ejcb

Research paper

Glypican-3 (GPC3) inhibits metastasis development promoting dormancy in breast cancer cells by p38 MAPK pathway activation

Macarena Guereño[a,1], Magali Delgado Pastore[a,1], Ana Clara Lugones[a], Magalí Cercato[a,b], Laura Todaro[a,b,1], Alejandro Urtreger[a,b,1], María Giselle Peters[a,b,*]

[a] Universidad de Buenos Aires, Instituto de Oncología A.H. Roffo, Área Investigación, Buenos Aires, Argentina
[b] CONICET

ARTICLE INFO

Keywords:
Breast cancer
Dormancy
Epithelial-to-mesenchymal transition
GPC3
Metastasis
p38 MAPK

ABSTRACT

GPC3 is a proteoglycan involved in the control of proliferation and survival, which has been linked to several tumor types. In this respect, we previously demonstrated that normal breast tissues exhibit high levels of GPC3, while its expression is diminished in tumors. However, the role of the GPC3 downregulation in breast cancer progression and its molecular and cellular operational machineries are not fully understood.

In this study we showed that GPC3 reverts the epithelial-to-mesenchymal transition (EMT) underwent by mammary tumor cells, blocks metastatic spread and induces dormancy at secondary site. Using genetically modified murine breast cancer cell sublines, we demonstrated that the phospho-Erk/phospho-p38 ratio is lower in GPC3 reexpressing cells, while p21, p27 and SOX2 levels are higher, suggesting a dormant phenotype. *In vivo* metastasis assays confirmed that GPC3 reexpressing cells reduce their metastatic ability. Interestingly, the presence of dormant cells was evidenced in the lungs of inoculated mice. Dormant cells could reactivate their proliferative capacity, remain viable as well as tumorigenic, but they reentered in dormancy upon reaching secondary site. We also proved that GPC3 inhibits metastasis through p38 pathway activation. The *in vivo* inhibition of p38 induced an increase in cell invasion of GPC3 reexpressing orthotropic tumors as well as in spontaneous and experimental metastatic dissemination.

In conclusion, our study shows that GPC3 returns mesenchymal-like breast cancer cells to an epithelial phenotype, impairs *in vivo* metastasis and induces tumor dormancy through p38 MAPK signaling activation. These results help to identify genetic determinants of dormancy and suggest the translational potential of research focusing in GPC3.

1. Introduction

Breast cancer is the neoplasia with the highest incidence as well as the main reason of cancer death in women (Torre et al., 2017). Even though many clinical therapies for reducing breast cancer mortality have been developed, metastasis still remains inadequately treated (Lorusso and Ruegg, 2012).

The epithelial-to-mesenchymal transition (EMT) is an embryonic procedure restated in carcinoma cells for metastasizing (Buchanan et al., 2011). Through this, cells of epithelial phenotype develop several properties of mesenchymal ones, as loss of homotypic adhesion, formation of actin stress fibers, increased migratory and invasive abilities, lower levels of epithelial protein– like E-Cadherin - as well as expression of mesenchymal markers, including vimentin (Gonzalez and Medici, 2014). Different signals activate the EMT-inducing transcription factors such as Snail1, Snail2 (SLUG), ZEB1 and ZEB2 (SIP1) among others. These factors repress the E-Cadherin expression, the main marker of the epithelial lineage. Additionally, the EMT process can be blocked by others transcription factors - which induce MET- like GRHL2 and ELF5, several microRNA (miR) families and p53 (De Craene and Berx, 2013). When these tumor cells invade contiguous tissues and reach circulation, they can continue viable as circulating tumor cells (CTCs), before extravasation at remote sites and the formation of the secondary tumors or metastatic foci (Buchanan et al., 2011). Importantly, some disseminated tumor cells (DTCs) are able to keep at distant organs under a viable and non-dividing status (Aguirre-Ghiso,

* Corresponding author at: Universidad de Buenos Aires, Instituto de Oncología A.H. Roffo, Área Investigación, CONICET, Av. San Martín 5481, (C1417DTB), Buenos Aires, Argentina.
E-mail addresses: mpeters@fmed.uba.ar, mgpeters@hotmail.com (M.G. Peters).
[1] Equal contribution.

https://doi.org/10.1016/j.ejcb.2020.151096
Received 26 November 2019; Received in revised form 20 May 2020; Accepted 9 June 2020

2006). *Dormancy* is the term employed to describe the latent reversible condition of these DTCs (Dittmer, 2017). Although the mechanism involved in latent cells awakening that leads to local recurrence as well metastasis development is not fully understood, it is suggested that the acquisition of mutations together with microenvironmental changes might induce it (Norkin et al., 2011). Several markers were associated with dormancy, such as low ratio of phospho-Erk / phospho-p38 (Aguirre-Ghiso et al., 2003), high expression of the cell cycle inhibitors p27 (Bragado et al., 2013) and p21 (Kobayashi et al., 2011), and up-regulation of pluripotency related transcription factors like NANOG, NR2F1, SOX9 and SOX2 (Sosa et al., 2015).

Proteoglycans (PGs) are a diverse glycoconjugates group, composed of different post-translationally modified proteins with one or more glycosaminoglycan chains (GAGs). Heparan sulfate (HS) and chondroitin sulfate (CS) are the two most common forms of sulfated GAGs. Among heparan sulfate proteoglycans (HSPG) is Glypican-3 (GPC3). We determined that this PG is extensively present in the embryo during morphogenesis and that its levels change in stage- and tissue-specific manner (Iglesias et al., 2008). However, GPC3 persists only in few adult tissues, like mammary gland (Pellegrini et al., 1998). Numerous studies have associated GPC3 with cell proliferation and apoptosis control (Filmus et al., 2008), and changes in its expression have been reported in cancer (Filmus, 2001). Interestingly, deregulation of GPC3 expression can both inhibit and promote tumor progression, depending on the cellular context (Stigliano et al., 2009). In general, GPC3 is overexpressed in tumors originated from GPC3-negative adult tissues, whereas it is downregulated in tumors arising from GPC3-positive adult tissues (Filmus and Selleck, 2001). So, several tumors overexpress GPC3, like hepatocarcinoma (Capurro et al., 2003), Wilms (Toretsky et al., 2001) and yolk sac tumors (Sugimura et al., 2004), although this glypican is downregulated in others, such as ovarian (Lin et al., 1999), gastric (Han et al., 2016), lung (Kim et al., 2003) and renal (Valsechi et al., 2014) tumors, as well as mesothelioma (Murthy et al., 2000). Our group analyzed human mammary gland, demonstrating the positive expression of GPC3 in normal tissues, although it was not found in tumors (Castillo et al., 2015). While GPC3 is downregulated in mammary tumors, we showed that its reexpression in murine (Peters et al., 2003) and human (Castillo et al., 2016) mammary cancer cell lines inhibits invasion and metastasis. We recently reported the complex connections through which the GPC3-regulated pathways are linked (Fernandez et al., 2018). While GPC3 modulates Wnt pathway, it has opposite effects depending on tumor type. Thus, GPC3 activates canonical Wnt signaling in hepatocarcinomas and promotes tumor progression (Capurro et al., 2005). On the other hand, we analyzed breast tumors and showed that GPC3 inhibits the β-Catenin/Wnt and PI3K/AKT pathways as well as activates the Wnt/PCP and p38 ones (Buchanan et al., 2010; Castillo et al., 2016; Stigliano et al., 2009). Altogether, this data suggests a metastasis suppressor role for GPC3 in the tumor mammary pathology (Buchanan et al., 2011).

It was shown that metastasis suppressors affect different phases of the metastatic process and several of them induce dormancy at the secondary site (Horak et al., 2008). Related to the putative function of GPC3 as metastasis suppressor, in this work we corroborated that it reverts the EMT underwent by murine mammary tumor cells. GPC3 reexpressing cells modulate their actin cytoskeleton structure, exhibit a 3D glandular-like arrangement, express the epithelial marker E-Cadherin while lose the mesenchyme-associated protein vimentin, reduce the expression of EMT-inducing transcription factors Snail1 and ZEB1, and are less metastatic. Interestingly, we showed that the phospho-Erk / phospho-p38 ratio is lower in LM3-GPC3 cells, whereas p21, p27 and SOX2 protein levels are higher, suggesting a dormant phenotype. Importantly, the presence of dormant cells was evidenced in lungs from intravenously injected mice. These dormant LM3-GPC3 cells reactivate their proliferative capacity, remain viable, tumorigenic, but they re-enter in dormancy upon reaching secondary colonization site. Our studies imply GPC3 in breast tumor dormancy activation through a system involving p38 MAPK. Although the *in vivo* inhibition of p38 does not affect the tumor growth, it induces an increase in local invasion of GPC3 reexpressing tumors, as well as in spontaneous and experimental metastatic dissemination.

The EMT and dormant DTCs greatly complicate therapeutic strategies, thus studying these processes serves as relevant approaches for cancer treatment. Here we show a previously unrecognized GPC3 mechanism, where DTCs dormancy is regulated through the p38 MAPK signaling pathway activation.

2. Materials and methods

2.1. Cell lines and culture proceedings

In this work we employed 4 cell sublines, derived of the murine metastatic mammary adenocarcinoma cell line called LM3 (ER -, PR -, Her2 +, GPC3 -) (Urtreger et al., 1997). LM3 cells were transfected using pEF-BOS (Mizushima and Nagata, 1990) with the Hemagglutinin A (HA)-tagged OCI-5/GPC3 cDNA or with the empty plasmid (Filmus et al., 1995). After 400 μg/mL G418 (Gibco Life Technologies, Carlsbad, CA, USA) antibiotic selection, transfected cells were cloned. We generated two sublines expressing GPC3 (LM3-GPC3 #1 and LM3-GPC3 #2) and two control sublines (LM3-vector #1 and LM3-vector #2) (Peters et al., 2003).

All cells were maintained at 37 °C, 5% CO_2, in minimum essential medium (MEM) (41,500 Gibco Life Technologies, Carlsbad, CA, USA), plus non-essential amino acids, 2 mM L-glutamine, 5% fetal calf serum (FCS) (Internegocios, Buenos Aires, Argentina) and 80 μg/mL gentamicin. Hoechst's staining and qPCR were regularly employed to check mycoplasma-free status.

2.2. In vitro pharmacological p38 inhibitor treatment

LM3-GPC3 cells were cultured 24 h without FCS, and then incubated for additional 48 h with 15 μM SB203580 or DMSO (vehicle) as control. This drug inhibits p38 catalytic activity by attaching to the ATP binding pocket, although it does not inhibit phosphorylation of p38 by upstream kinases (Kumar et al., 1999). RNA from treated cells was extracted and analyzed by qPCR to determine p53 and p21 expression levels.

2.3. Primary cultures

Lungs without metastatic nodules from mice intravenously inoculated with LM3-GPC3 sublines or lungs with metastasis from mice injected with LM3-vector cells were dissected. Sterile phosphate-buffered saline (PBS) was employed twice for washing the samples, which were cut into small pieces of 1 mm. The fragments were incubated with dissociative enzymes (Pronase 0.01 %, DNAse 2.4 mg/mL) during 30 min at 37 °C in agitation. Supernatants were then recovered, and the undigested fragments were incubated with Pronase-DNAse solution for additional 30 min. After the second digestion, the supernatant was collected, combined with the first one and centrifuged at 150xg during 10 min. Pellets were resuspended in MEM (41,500 Gibco Life Technologies, Carlsbad, CA, USA), 10 % FCS (Internegocios, Buenos Aires, Argentina) plus 80 μg/mL gentamicin, and incubated in a petri dish. After 24 h, new MEM was placed and 400 μg/mL G418 (Gibco Life Technologies, Carlsbad, CA, USA) was added for selecting resistant tumor cells. Primary cultures were maintained in the presence of the antibiotic in the successive passages.

2.4. Cell morphology

LM3-GPC3 and LM3-vector sublines, as well as primary cultures were analyzed in a NIKON Eclipse E-400 microscope (Nikon Corporation, Tokyo, Japan) by phase contrast. Representative Bright

Field (BF) images were taken.

2.5. Actin cytoskeleton organization

For F-Actin staining, cells were seeded on coverslips. When they reached subconfluence, were washed with PBS and fixed in 0.4 % paraformaldehyde during 15 min at RT. Cells were cleaned again and then permeabilized employing 0.2 % Triton X-100 in PBS. Following 3 additional washes, monolayers were incubated with Phalloidin-Alexa 546 (1:500, Sigma-Aldrich, St. Louis, MO, USA) during 45 min. Mowiol 4–88 (Sigma-Aldrich, St. Louis, MO, USA) was used to mount the coverslips. All procedures were performed in the dark. Fluorescence images were captured by a NIKON Eclipse E-400 fluorescence microscope (Nikon Corporation, Tokyo, Japan).

2.6. Non-adherent cell growth

To study the ability to form spheroids, 3 10^4 LM3-GPC3 or LM3-vector clones were cultured in 24-well plate coated with 1 % agar (Gibco LifeTechnologies, Carlsbad, CA, USA), in medium with 10 % FCS. On the seventh day, cell aggregates were evaluated under NIKON Eclipse E-400 microscope (Nikon Corporation, Tokyo, Japan). Additionally, 0.4 % paraformaldehyde was used during 15 min to fix cell clusters. Then, they were washed two times with PBS and stained overnight employing 20 mg/mL propidium iodide in 0.1 % citrate buffer-0.1 % Triton X-100. Cell aggregates were evaluated under Carl Zeiss LSM 5 Pascal confocal microscope (Carl Zeiss AG, Oberkochen, Germany) and representative images were taken.

2.7. Western blotting

PBS was used three times to wash subconfluent monolayers. Next, they were incubated in lysis Buffer (1 % Triton X-100/PBS) plus protease inhibitors mix (Sigma-Aldrich, Saint Luis, MO, USA), during 45 min at 4 °C in agitation. Samples were centrifuged at 15,000xg for 15 min at 4 °C and supernatants were conserved.

Total protein concentration was determined by Bradford method. The extracts were heated in Laemmli buffer plus 10 % β-mercaptoethanol. SDS-PAGE was utilized to separate proteins, which were shifted (0.6 A; 60 min) to PVDF membrane (Hybond-P, Amersham-GE Healthcare, Little Chalfont, Buckinghamshire, UK) by "Mini Trans-Blot module" (Bio-Rad, Hercules, CA, USA). Non-specific binding was prevented through the incubation of membranes in 5 % non-fat milk or 5 % BSA, 0.05 % Tween-20–Tris buffer saline (TTBS), for 1 h at RT. The following primary antibodies were used overnight: anti-HA Tag (for GPC3 detection, 1:500, Santa Cruz Biotechnology, Dallas, TX, USA), anti-E-Cadherin (1:500, BD Bioscience, San Jose, CA, USA), anti-Snail (1:1000, Cell Signaling, Danvers, MA, USA), anti-ZEB1 (1:500, Cell Signaling, Danvers, MA, USA), anti-Vimentin (1:500; Santa Cruz Biotechnology, Dallas, TX, USA), anti-p38 (1:500; Santa Cruz Biotechnology, Dallas, TX, USA), anti-phospho p38 (1:200; Santa Cruz Biotechnology, Dallas, TX, USA), anti-Erk1/2 (1:500; Santa Cruz Biotechnology, Dallas, TX, USA), anti-phospho Erk1/2 (1:500; Santa Cruz Biotechnology, Dallas, TX, USA), anti-p21 (1:200; Santa Cruz Biotechnology, Dallas, TX, USA), anti-p27 (1:200; Santa Cruz Biotechnology, Dallas, TX, USA), anti-SOX2 (1:500; Abcam, Massachusetts, USA), anti-OCT 4 (1:500; Abcam, Massachusetts, USA), anti-NANOG (1:500; Abcam, Massachusetts, USA), anti-α-Tubulin (1:500; Abcam, Massachusetts, USA) and anti-β-Actin (1:5000, Sigma-Aldrich St. Louis, MO, USA). Membranes were washed three times in TTBS and then incubated during 1 h at RT with horseradish peroxidase-labeled secondary antibodies goat anti-mouse (1:5000, Santa Cruz Biotechnology, Dallas TX, USA) or goat anti-rabbit (1:5000, Sigma-Aldrich St. Louis, MO, USA). To visualize bands, a chemiluminescent reagent was employed. Images were obtained in a camera system for chemiluminescence (ImageQuant LAS 500 chemiluminescence CCD camera, GE, Schenectady, USA) and bands were densitometrically evaluated (ImageJ1.49 m program).

2.8. PCRs (RT-PCR: reverse transcription polymerase chain reaction. qPCR: quantitative polymerase chain reaction)

We obtained total RNA using TRI Reagent® (TR 118-Molecular research Center, INC., Cincinnati, OH, USA). NanoDrop2000 spectrophotometer (Thermo Fisher Scientific, Waltham, MA, USA) was utilized to quantify RNA and to analyze purity through the determination of 260/280 nm absorbance. Samples quality was evaluated by agarose gel.

For cDNA synthesis, reverse transcriptions were done. The reaction mixes - 1 μg RNA treated with 1 unit DNase I (Thermo Fisher Scientific, Waltham, MA, USA) and iScript cDNA Synthesis Kit (Bio-Rad, Hercules, CA, USA) - were incubated for 5 min at 25 °C, 20 min at 46 °C and 1 min at 95 °C. The synthesized cDNA was treated with 1 unit RNase H (Amersham-GE Healthcare, Little Chalfont, Buckinghamshire, UK), diluted in TE buffer and stored at −20 °C.

RT-PCR was done to evaluate if LM3 sublines were able to express GPC3. The reactions included: 1.5 μL cDNA, forward and reverse primers for GPC3 or GAPDH (GPC3 Fw 5´GGAAGAAGGGAACTGATT CAG3´, Rv 5´CACATCCAGATCATATGCCAG3´; GAPDH Fw 5´TGCACC ACCAACTGCTTAGC3´, Rv 5´GGCATGGACTGTGGTCATGAG3´), 2 units of Taq Polymerase (Thermo Fisher Scientific, Waltham, MA, USA), 50 mM MgCl and 1 mM dNTPs. We followed the protocol: 4 min at 94 °C, 27 cycles at 94 °C during 50 s at 55 °C and 1 min at 72 °C and one cycle at 72 °C during 7 min. The same reaction was done employing positive and negative controls. Agarose gels plus ethidium bromide were utilized to analyze the reaction results.

qPCR was performed using the RT–PCR Kit (5x HOT FIREPol EvaGreen qPCR Mix Plus, no ROX, Solis BioDyne, Tartu, Estonia). Reactions contained: 2 μL cDNA (1:3), 5 μL 5x HOT FIREPol EvaGreen, as well as forward and reverse primers (p21: Fw 5´GTCTGAGCGGCCT GAAGATTC3´ Rv 5´TTCAGGGTTTTCTCTTGCAGAAG3´; p53: Fw 5´ CGACCTATCCTTACCATCATCACA3´ Rv 5´CACAAACACGAACCTCAAA GCT3´; E-Cadherin: Fw 5´GCTCTCATCATCGCCACAG3´ Rv 5´CTGGGA TGGGAGCGTTGTC3´; Vimentin: Fw 5´GAGATCGCCACCTACAGGAA3´ Rv 5´TCCATCTCTGGTCTCAACCG3´; GAPDH: Fw 5´TGCACCACCAAC TGCTTAGC3´ Rv 5´GGCATGGACTGTGGTCATGAG3´; HPRT Fw 5´ CTGGTGAAAAGGACCTCTCGAAG3´ Rv 5´CCAGTTTCACTAATGACAC AAACG3´). PCR was done in a Bio-Rad C1000 Thermal Cycler (Bio-Rad, Hercules, CA, USA) as follows: 2 min at 50 °C, 15 min at 95 °C, and 40 cycles at 95 °C for 15 s, 20 s at 60 °C and 30 s at 72 °C. The $2^{-\Delta\Delta Ct}$ equation was utilized to obtain the relative mRNA levels of each gene. Biological and technical replications were completed two or three times.

2.9. In vivo assays

2.9.1. Animals

Assays were performed with 8-weeks old BALB/c female mice (Instituto de Oncología "A. H. Roffo"). The study accompanied ethical standards, following ARRIVE (Animal Research: Reporting of *In Vivo* Experiments) procedures. The Animal Care and Use Committee of the Universidad de Buenos Aires (CICUAL) approved these experiments. A maximum of 5 animals were housed per cage, which were kept in a 12 h dark / light regime, with water and food in pellets on demand.

2.9.2. Dormancy evaluation

2.9.2.1. Experimental lung metastasis. Mice (5 per experimental group) were intravenously injected in the tail vein with 3 10^5 LM3-GPC3 or LM3-vector cells, in 0.2 mL of MEM. After 21 days, animals were euthanized; their lungs were removed, rinsed in PBS and analyzed under a dissecting microscope. Metastatic nodules were recorded and expressed as median (Md) and range (Rg). Some lungs were reserved for primary cultures.

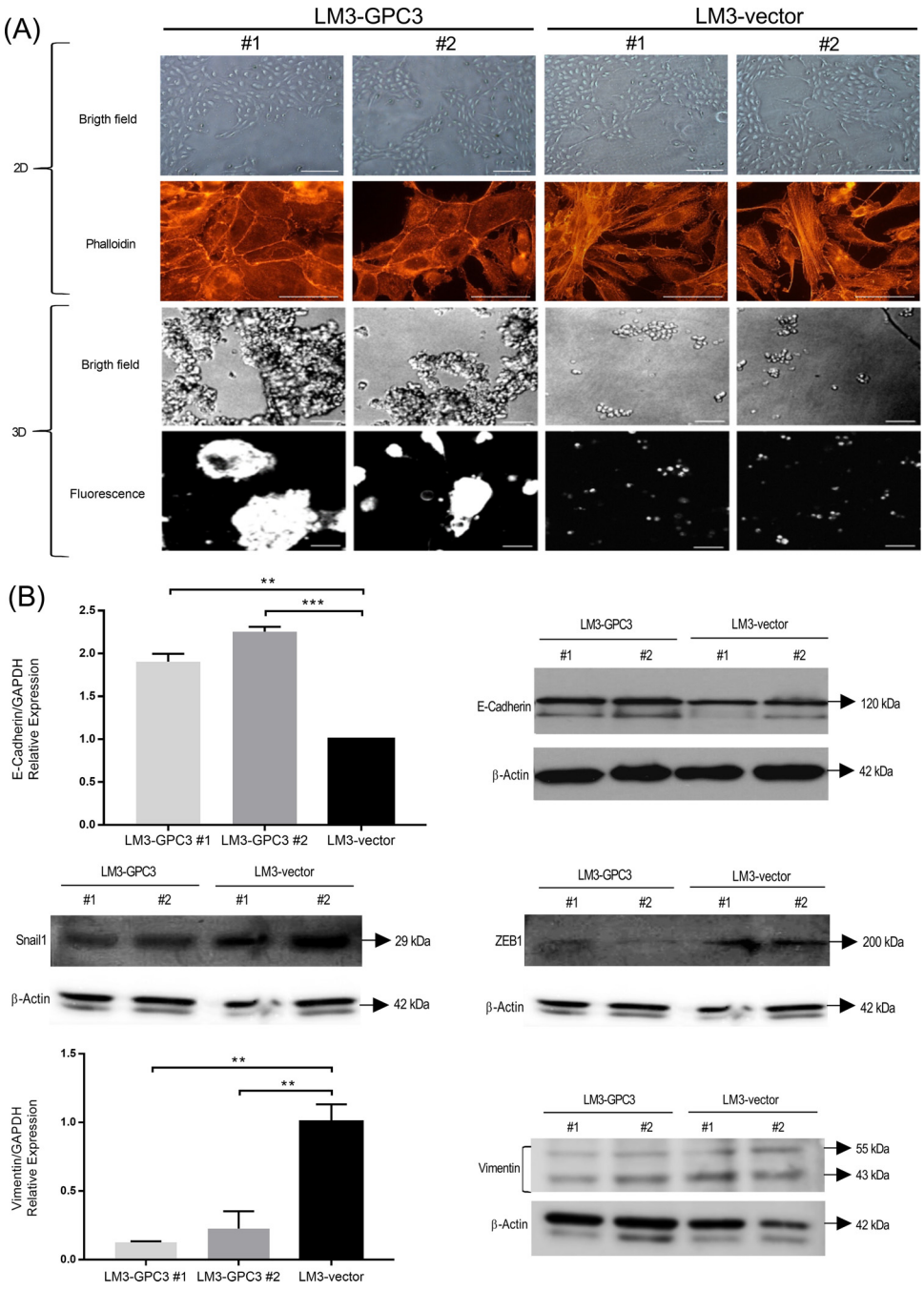

Fig. 1. Effects of GPC3 on cell growth, actin cytoskeleton organization and EMT markers expression. (A) Morphological and growth cell characteristics. *Top panel*: 2D culture. Cells were grown on coverslips and bright field (BF) images were taken (scale bars 100 μm). To study the actin cytoskeleton, cells were stained with phalloidin-Alexa 546 and analyzed under fluorescence microscope (scale bars 50 μm). Images are representative of three independent experiments. *Bottom panel*: 3D culture. Cells were seeded in plates coated with 1 % agar. After 7 days growing in suspension, the cell aggregates were evaluated under microscope (scale bars 100 μm). Additionally, spheroids were stained with propidium iodide and evaluated under confocal microscopy. Photographs were taken (scale bars 100 μm). Images are representative of three independent experiments. (B) EMT markers expression. *Top panel, Left:* E-Cadherin mRNA expression levels were quantified by qPCR and GAPDH was used as an internal control. Bars represent mean values ± SD (*** $p < 0.001$, ** $p < 0.005$ ANOVA, Tukey´s multiple comparisons tests). *Right:* WB analysis was employed to determine E-Cadherin protein expression. β-Actin was used as control. Numbers on the right represent molecular mass (kDa). *Middle panel:* Representative images of Snail1 (*left*), ZEB1 (*right*) and β-Actin (control) WBs are shown. *Bottom panel, Left:* Vimentin mRNA levels were determined using qPCR. Bars represent mean values ± SD (** $p < 0.005$ ANOVA, Tukey´s multiple comparisons tests). *Right:* Vimentin protein levels were analyzed by WB. β-Actin was employed as seeding control. All showed experiments are representative of two or three independent ones.

2.9.2.2. Subcutaneous tumor. Animals (5 per experimental group) were subcutaneously injected in the left flank with 4 10^5 "ex dormant" primary culture cells, in 0.3 mL of MEM. Latency (days for the first tumor palpation after injection) and tumorigenicity (number of animals that developed tumors respect the total number of animals injected; %, n/n) were registered. Tumor growth was monitored twice a week by measuring with caliper the major and minor diameters and expressed as volume ($V = 0.5 \times d^2 \times D$ (D long; d short diameters). We did growth curves for each experimental group, from which the tumor growth rate was obtained (expressed as cm^3/day).

Tumor-bearing mice were euthanized at 35 days post-inoculation or when tumor size exceeded ethical standards, or when the animal presented symptoms of pain. Necropsy was performed with special interest in search metastatic foci in lungs and lymph nodes. Lungs were removed and observed under a dissecting microscope. The number of spontaneous metastatic nodules was recorded and expressed as median (Md) and range (Rg). The metastasis incidence was also calculated and showed as the number of mice displaying lung nodules based on the total number of animals of the corresponding experimental group (%, n/n). Some lungs were also preserved for primary culture.

2.9.3. In vivo p38 MAPK modulation

2.9.3.1. Experimental lung metastasis. Mice (5 for each experimental group) intravenously inoculated in the tail vein with 3 10^5 LM3-GPC3 and LM3-vector clones, were simultaneously injected with 10 mg/kg SB203580 (p38 MAPK inhibitor) or with vehicle (DMSO). The drug or vehicle was administered once a day for 5 days. After 21 days animals were euthanized, and the number of experimental lung metastatic nodules was recorded and presented as median (Md) and range (Rg).

2.9.3.2. Subcutaneous tumor. 24 h post subcutaneous inoculation of 4 10^5 LM3-GPC3 and LM3-vector cells, animals (5 for each experimental

group) were intraperitoneally treated with 10 mg/kg SB203580 or with DMSO. The drug or vehicle was administered once a day for 10 days.

Latency (days for the first tumor palpation after injection) and tumorigenicity (number of animals that developed tumors respect the total number of animals injected; %, n/n) were registered. Tumor growth was monitored twice a week as was above described. Briefly, the major and minor diameters were measured by caliper and expressed as volume ($V = 0.5 \times d^2 \times D$ (D long; d short diameters). Tumor growth rate was obtained (expressed as cm^3/day) from growth curves of each experimental group. Macroscopic local invasion (ulceration) was analyzed and expressed as the number of animals with local invasion respect to the total number of animals (%, n/n). 30 days post-inoculation or when tumor size exceeded ethical standards, or when the animal presented symptoms of pain, mice were euthanized, and necropsy was performed. The number of spontaneous lung metastatic foci was recorded and presented as median (Md) and range (Rg).

2.10. Statistical analysis

Graph Pad Prism 8 was used to statistical analysis. Power calculation (Mann Whitney *U* test did at 90 % power at 5% significance) indicated that $n = 5$ animals are suitable for statistical significance. Mice were assigned to treatment groups by random sampling. The comparisons of tumor and metastatic incidence as well as macroscopic and microscopic invasion data were done by chi-square test. Kruskal-Wallis and Dunn´s tests were used to analyze difference among number of metastatic nodules as well as tumor growth rates. Subcutaneous tumor growth was tested employing exponential growth equation comparisons.

The results are shown as mean ± SD, considering $p < 0.05$ as significant, and represent leastwise two independent assays.

3. Results

3.1. GPC3 reexpression induces alterations in morphology, 3D growth properties as well as in epithelial and mesenchymal gene expression

LM3-GPC3 #1 and LM3-GPC3 #2 sublines were obtained from LM3 murine mammary adenocarcinoma cell line by transfection with a plasmid containing the GPC3 cDNA and then cloned. Additionally, LM3-vector #1 and LM3-vector #2 control cell sublines were generated by transfecting with an empty plasmid (Peters et al., 2003). These cell sublines share several features of human HER2-positive breast cancer tumors (RE-, RP-, Her2+). As shown in Fig. S1, while LM3-vector cells did not express GPC3, this glypican was detected both at mRNA (Fig. S1A) and protein (Fig. S1B) levels in LM3-GPC3 sublines (periodically checked).

We previously determined that GPC3 modulates several tumor properties acquired by LM3 cells (Peters et al., 2003). We confirmed that both GPC3 reexpressing and control sublines growth as epithelial adherent cells in two-dimensional (2D) culture (Fig. 1A). Via phalloidin-Alexa 546 staining it was proved that GPC3 reexpression induces the loss of F-actin stress fibers, which were present in control clones (Fig. 1A). Moreover, we showed that when cells are grown on three-dimensional culture (3D), LM3-vector sublines are unable to form spheroids, or they only establish small colonies with poor/null cell-cell contacts. However, LM3-GPC3 cells exhibited this ability (Fig. 1A). In addition, we analyzed the structural organization of these 3D clusters. We determined by propidium iodide staining and confocal fluorescence microscopy, that LM3-GPC3 cell aggregates form lumens (Fig. 1A). This organization is typical of normal mammary epithelial cells. LM3-vector cell clusters did not arrangement these glandular-like structures. Therefore, our data reinforces the hypothesis that this glypican leads to a more normal epithelial phenotype, modifying the mesenchymal properties acquired by LM3 cells. So, we proposed to complete the analysis of the potential function of GPC3 in the EMT process. We confirmed, by qPCR and WB, our earlier findings showing higher E-Cadherin levels in GPC3 reexpressing cells (Fig. 1B, top panel. $p < 0.001$ ANOVA). In agreement, we also found that the expression of Snail1 and ZEB1 -two transcription factors involved in E-Cadherin downregulation- is decreased in LM3-GPC3 sublines (Fig. 1B, middle panel). Given the regulation of these EMT markers, we also examined the levels of vimentin. We found that GPC3 induces a reduction in this mesenchymal marker, both at mRNA and protein levels (Fig. 1B, bottom panel. $p < 0.05$ ANOVA). These results, together with our previous ones, support the idea that GPC3 is reversing EMT suffered by mammary tumor cells.

3.2. GPC3 reexpression induces in vivo dormancy at the secondary tumor site

Data presented in Fig. 1, as well as an exhaustive analysis of the murine sublines previously performed (Buchanan et al., 2010; Fernandez et al., 2018; Peters et al., 2003; Stigliano et al., 2009), led to postulate that this glypican acts as a breast cancer metastasis suppressor (Buchanan et al., 2011). In addition, we also determined that GPC3 suppresses metastasis in human mammary tumor models (Castillo et al., 2016). Despite our consistent evidences, there is not a complete description of the GPC3 suppressive activity system.

It has been proposed that many metastasis suppressors promote dormancy at the secondary site. Several authors have reported that a decreased activity ratio of Erk to p38 determinates cellular dormancy (Aguirre-Ghiso et al., 2003; Kobayashi et al., 2011; Lenk et al., 2017). Since we previously informed that GPC3 modulates p38 MAPK pathway activity (Buchanan et al., 2010; Fernandez et al., 2018), we decided to calculate the phospho-Erk / phospho-p38 ratio in our cellular model. As is shown in Fig. 2A, GPC3 reexpression did not induce any changes in Erk phosphorylation levels. However, p38 phosphorylation was increased in LM3-GPC3 cells. Thus, the Erk / p38 activity ratio was decreased by GPC3 reexpression. Similarly, the cell cycle inhibitors p21 and p27 were previously considered as dormancy markers (Bragado et al., 2013; Kobayashi et al., 2011). In agreement, we found higher basal p21 and p27 protein levels in LM3-GPC3 cell sublines (Fig. 2B). It was also described that transcription factors initially defined in stem cells from embryos can induce dormancy (Sosa et al., 2015). So, here were evaluated SOX2, NANOG and OCT4 expression levels. Although no signal was found for NANOG and OCT4 (data not shown), we detected a moderate upregulation at protein level of SOX2 in LM3-GPC3 cell sublines (Fig. 2C). Altogether, our data indicate that breast cancer cells exhibit dormant phenotype as a result of GPC3 reexpression.

Therefore, we performed *in vivo* assays to test whether GPC3 induces metastasis suppression by maintaining the disseminated cell in a dormant state. First, mice were intravenously injected with LM3-GPC3 and LM3-vector cell sublines. In association with already presented results (Peters et al., 2003), multiple metastatic lung foci were found in LM3-vector-injected animals. In contrast, LM3-GPC3 cells significantly reduced their ability to form lung metastasis (Fig. 3, $p < 0.005$ Kruskal-Wallis test). GPC3 induced a decrease in metastasis incidence, since only 20 % of mice inoculated with GPC3 reexpressing cells showed lung metastasis, while 100 % of animals inoculated with control sublines did it ($p < 0.005$ chi-square test).

Next, we aimed to determine whether lungs of LM3-GPC3-inoculated mice has dormant tumor cells. For this, lungs from mice inoculated with GPC3 reexpressing cells (without metastasis), and lungs from mice injected with control sublines (with macroscopic metastatic foci) were cultured (Fig. 3). After 21 days of selection with 400 μg/mL of G418, only antibiotic resistant LM3-vector or LM3-GPC3 cells remained in the cultures. Surprisingly, despite that metastatic foci were not detected, the presence of LM3-GPC3 cells was confirmed in primary cultures. These results agree with the fact that dormancy is a reversible state, since when latent cells are cultivated, they resume their growth ability. We confirmed by RT-PCR that these dormant LM3-GPC3 cells

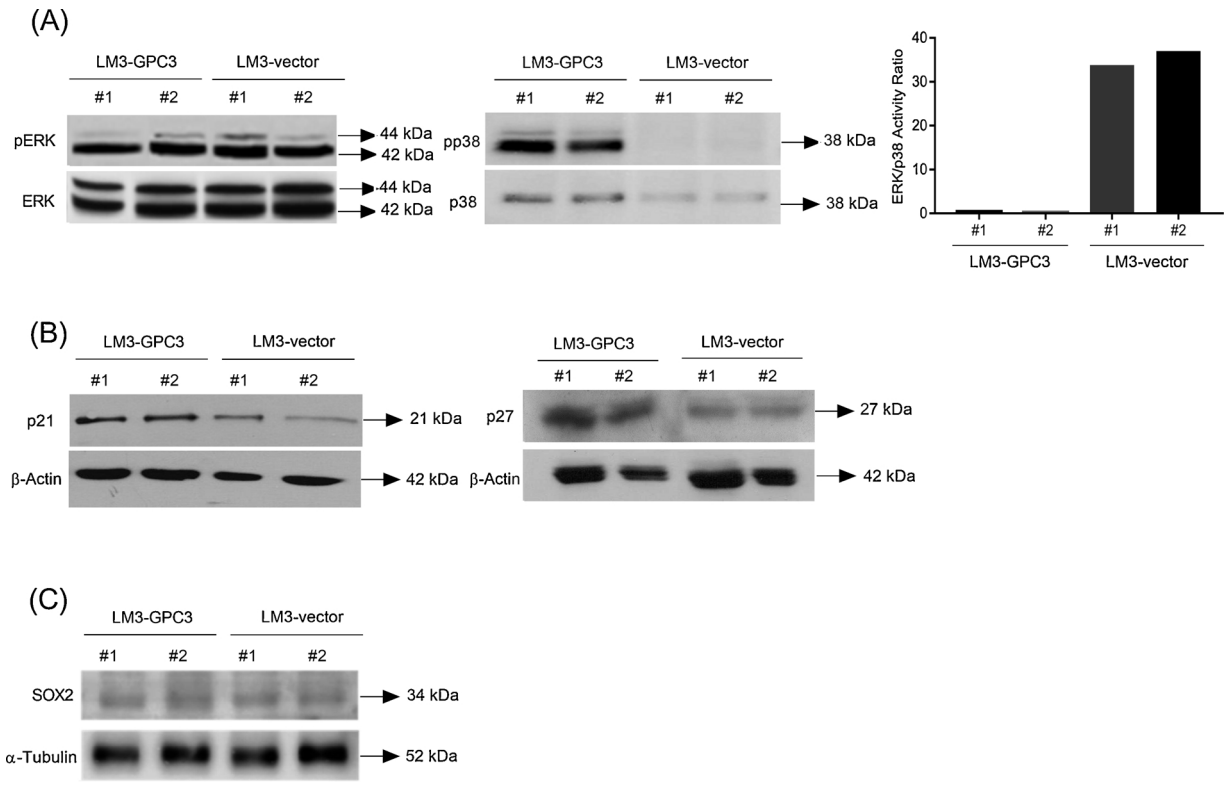

Fig. 2. Effects of GPC3 on dormancy markers expression. Total protein extracts were analyzed by WB. β-Actin or α-Tubulin was used as an internal control. Numbers on the right represent molecular mass (kDa). Representative images of three independent experiments are showed. (A) *Left panel*: phospho-Erk/Erk; *Middle panel*: phospho-p38/p38; *Right panel*: ratio of phospho-Erk to phospho-p38. (B) *Left panel*: p21; *Right panel*: p27. (C) SOX2.

still express the glypican (data not shown). Fig. 4A shows the morphological features of primary culture cells, which exhibited an epithelial appearance like their respective parental sublines (Fig. 1A). Moreover, by phalloidin-Alexa 546 staining we determined that LM3-GPC3 primary culture (or "ex dormant cells") organize their cytoskeleton similarly to the parental GPC3 reexpressing cells (Fig. 1A), locating actin at the cortical site. On the other hand, stress fibers were found in LM3-vector primary culture cells (Fig. 4A) like in the parental control ones (Fig. 1A). The expression of epithelial and mesenchymal markers was also checked. We confirmed, by qPCR and WB, that E-Cadherin levels are higher in LM3-GPC3 primary culture cells, while vimentin is reduced (Fig. 4B, $p < 0.005$ ANOVA test for E-Cadherin and vimentin qPCRs).

We postulate that GPC3 function is limited to dormancy. Consequently, its expression should not disturb tumor development. To test this, mice were subcutaneously inoculated with primary culture cells. As we previously determined with the parental sublines (Peters et al., 2003), LM3-vector and LM3-GPC3 primary culture tumors has comparable latency and growth rates (Table 1, ns Kruskal-Wallis test; Fig. 5, ns Exponential growth equation). LM3-GPC3 "ex dormant" cells were still viable and tumorigenic. Additionally, lung foci were studied for determining the spontaneous metastatic ability. We established that the number of macroscopic nodules is significantly lower in mice inoculated with GPC3 reexpressing primary culture cells (Table 1, $p < 0.005$ Kruskal-Wallis test). Moreover, the metastasis incidence was also lower. We found that all mice carrying primary culture control tumors develop metastasis, but only 20–40 % of LM3-GPC3 primary culture tumor- bearing mice exhibited lung metastatic nodes (Table 1, $p < 0.05$ chi-square test). Interestingly, we proved that lungs from primary culture LM3-GPC3 tumor-bearing mice that did not exhibit metastasis, has dormant cells. As was performed with parental sublines, lungs without metastatic foci were cultured and selected with 400 μg/mL of G418. The presence of LM3-GPC3 cells was confirmed. We also checked by RT-PCR that these dormant cells still express GPC3 (data not shown). In sum, LM3-GPC3 "ex dormant" cells enter in a dormant non-dividing sate at distant organ, but can cross the total of metastasis stages. We demonstrated that dormant LM3-GPC3 cells can reactivate their proliferative capacity, remain viable and tumorigenic, but they re-enter in a dormant state upon reaching secondary tumor colonization site.

3.3. GPC3 reexpression induces dormancy through p38 MAPK pathway activation

As was mentioned, we demonstrated that GPC3 inhibits breast cancer metastatic spread (Fig. 3, $p < 0.005$ Kruskal-Wallis test and (Peters et al., 2003). Given that a p38 signaling activation was detected in GPC3 reexpressing cells (Fig. 2A middle panel and (Buchanan et al., 2010; Fernandez et al., 2018) and since p38 determinates cellular dormancy (Aguirre-Ghiso et al., 2003; Kobayashi et al., 2011; Lenk et al., 2017), we next aimed to study whether GPC3 inhibits metastatic spread through the p38 MAPK activation.

As technical strategy we repressed the p38 MAPK signaling by employing the pharmacological inhibitor SB203580. First, we corroborated that this drug inhibits the p38 pathway activity in our cellular model. As seen in Fig. S2, the treatment with SB203580 significantly reduced the expression of the p38 transcriptional targets p53 and p21. Next, LM3-GPC3 or LM3-vector sublines were subcutaneously inoculated into BALB/c mice, and the p38 inhibitor SB203580 (or DMSO as control) was intraperitoneally administered for 10 days.

We determined that LM3-GPC3 and LM3-vector sublines generate subcutaneous tumors, which show similar latency and tumorigenic capacity, irrespective of SB203580 treatment (Table 2). In addition, the inhibition of p38 did not affect the LM3-vector nor LM3-GPC3 tumor growth (Table 2, ns Kruskal-Wallis test; Fig. 6A, ns Exponential growth equation). However, while only 20–40 % of LM3-GPC3 + DMSO

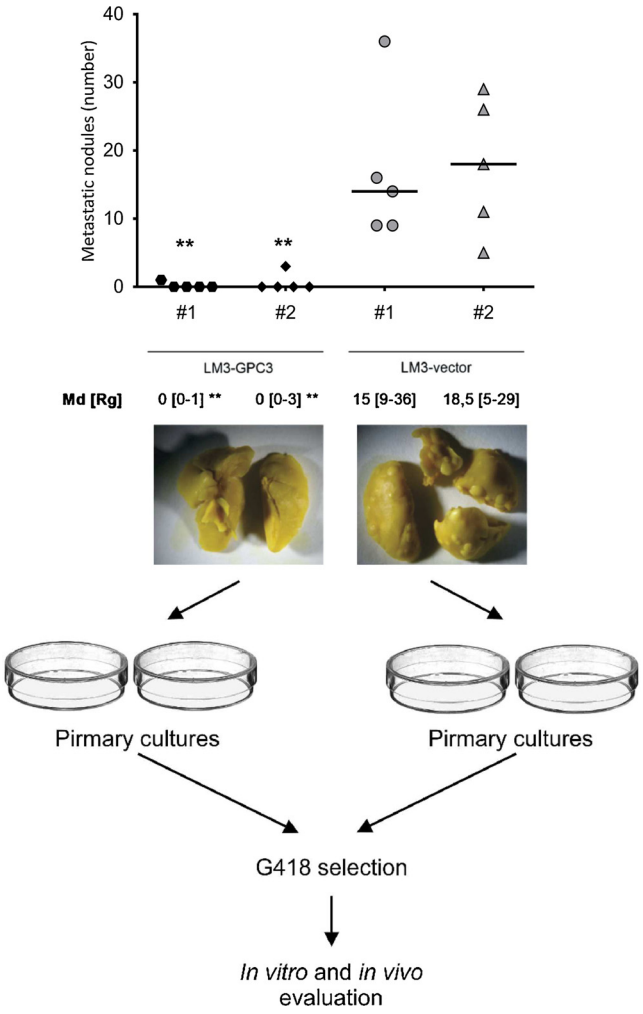

Fig. 3. Effects of GPC3 on *in vivo* metastatic outgrowth. LM3-GPC3 and LM3-vector cell sublines were intravenously inoculated into BALB/c mice (n = 5 animals per group) and after 21 days the number of metastatic lung foci was recorded. Median (Md) and range (Rg) are included, as well as illustrative photos of lungs. Schematic methodological proceeding is also shown. Data is representative of three independent experiments (** $p < 0.05$ Kruskal-Wallis, Dunn´s test).

tumors showed macroscopic invasion compared to 80 − 100 % of LM3-vector + DMSO ones, the SB203580 treatment increased the invasion and ulceration of GPC3 reexpressing tumors (reaching between 80 − 100 % of LM3-GPC3 tumors affected) (Table 2, $p < 0.05$ chi-square test). It is important to note that the SB203580 treatment did not have effect on invasion ability of LM3-vector control tumors.Furthermore, the histopathological study also exposed differences. In agreement with macroscopic observations, the drug did not affect the microscopic invasion of LM3-vector tumors. However, we demonstrated that the SB203580 treatment reverses the GPC3 inhibitory action on microscopic local invasion. While GPC3 reexpressing tumors rarely invaded the subcutaneous muscle and the dermis, the p38 inhibitor treated mice tumors did (Fig. 6B). By animals necropsy we determined that cell sublines exclusively colonize lungs irrespectively of the inhibitor treatment. While LM3-GPC3 tumor-bearing mice treated with vehicle showed less metastatic nodules than control animals (LM3-vector + DMSO), the SB203580 treatment reversed partially this inhibition (Table 2 and Fig. 6C, $p < 0.005$ Kruskal-Wallis test). The lungs macroscopic analysis confirmed that GPC3 blocks metastasis (Table 2, $p < 0.001$ chi-square test). Importantly, the p38 inhibitor induced a critical progress in LM3-GPC3 metastasis spread although it did not change control metastasis development. As is shown in Table 2, 60 % of mice carrying GPC3 reexpressing tumors treated with SB203580 were able to develop lung metastases (Table 2, $p < 0.05$ chi-square test). Additionally, the histopathologic study showed metastatic nodules in lungs of all LM3-GPC3 + SB203580, LM3-vector + DMSO and LM3-vector + SB203580 tumor-bearing mice, while no metastases were found in animals carrying LM3-GPC3 + DMSO tumors (Fig. 6 C lower panel). Our data suggest that GPC3 inhibits the metastasis spread of mammary tumor cells and induces dormancy at secondary site, through the p38 MAPK activation.

To confirm our idea, the experimental metastatic capacity was tested. LM3-GPC3 and LM3-vector cell sublines were intravenously inoculated into mice, which were simultaneously administered with SB203580 (alternatively DMSO) for 5 days. Our results showed that mice inoculated with LM3-GPC3 cells + SB203580 significantly increase the number of lung metastases, reaching levels like those detected in animals injected with LM3-vector cells (Table 2 and Fig. 6D, $p < 0.05$ Kruskal-Wallis test). Once again, the drug did not affect control cells metastatic colonization.

4. Discussion

Disseminated tumor cells (DTC) frequently resist systemic therapies and can lead to lethal metastatic lesions (Dittmer, 2017). The cellular phenotype plasticity plays a relevant function in metastasis from carcinomas of epithelial origin. Epithelial-to-mesenchymal transition (EMT) is the initial metastatic stage, through which tumor epithelial cells gain several characteristics of mesenchymal ones (Buchanan et al., 2011). With the aim to describe new molecules regulating the EMT process, here we deepen the analysis of GPC3. As we previously suggested (Castillo et al., 2016; Peters et al., 2003), we confirm that GPC3 reexpression induces the restructuring of actin cytoskeleton, with the loss of stress fibers developed by LM3 tumor cells. Furthermore, this glypican changes the 3D growth, activating the spheroids development. This result, that suggests the recovery of the epithelial junctions lost by LM3 cells, is in association with our previous report indicating that GPC3 modulates the capability of human mammary tumor MDA-MB231 cell line to proliferate in suspension, unattached to any substrate (Castillo et al., 2016), as well as with Gao et. al. who reported that the *in vitro* hepatocarcinoma spheroid formation is inhibited by blocking the heparan sulfate chains on GPC3 (Gao et al., 2015). Importantly, in this work we studied the 3D structure showing that LM3-GPC3 spheroids have hollow lumen. So, these GPC3 reexpressing cell clusters resemble normal breast architecture, recapitulating the mammary glandular lumen formation (Djomehri et al., 2019) and reverting the 3D phenotype acquired by LM3 cells during EMT. The GPC3 action on EMT has was also checked by the evaluation of molecular markers. We found that the epithelial marker E-Cadherin is upregulated in GPC3 reexpressing cells, while the mesenchymal one vimentin is downregulated. Furthermore, levels of Snail1 and ZEB1 transcription factors - capable of inducing EMT through E-Cadherin downregulation - were found decreased in LM3-GPC3 sublines. Altogether, this data stresses the close link between GPC3 and EMT working in tumor progression. Wu et. al. also connected GPC3 with EMT in hepatocarcinoma cells (HCC) (Wu et al., 2015). However, in association to the described activating role of GPC3 on *in vivo* and *in vitro* progression of HCC (Capurro et al., 2005; Zittermann et al., 2020), the authors found that this glypican promotes the transition. On the other hand, recent works reported the connection between GPC5 and EMT. GPC5 exhibits high homology to GPC3, and can inhibit the EMT in prostate cancer (Sun et al., 2018) as well as in lung adenocarcinoma (Wang et al., 2016), while it induces the transition in uterine carcinomas (Chui et al., 2018).

We hypothesize that GPC3 acts as a breast cancer metastasis suppressor (Buchanan et al., 2011; Peters et al., 2003), and inhibits the EMT. In association with the potential role of metastasis suppressors as tumor dormancy inductors (Nash et al., 2007), here it was

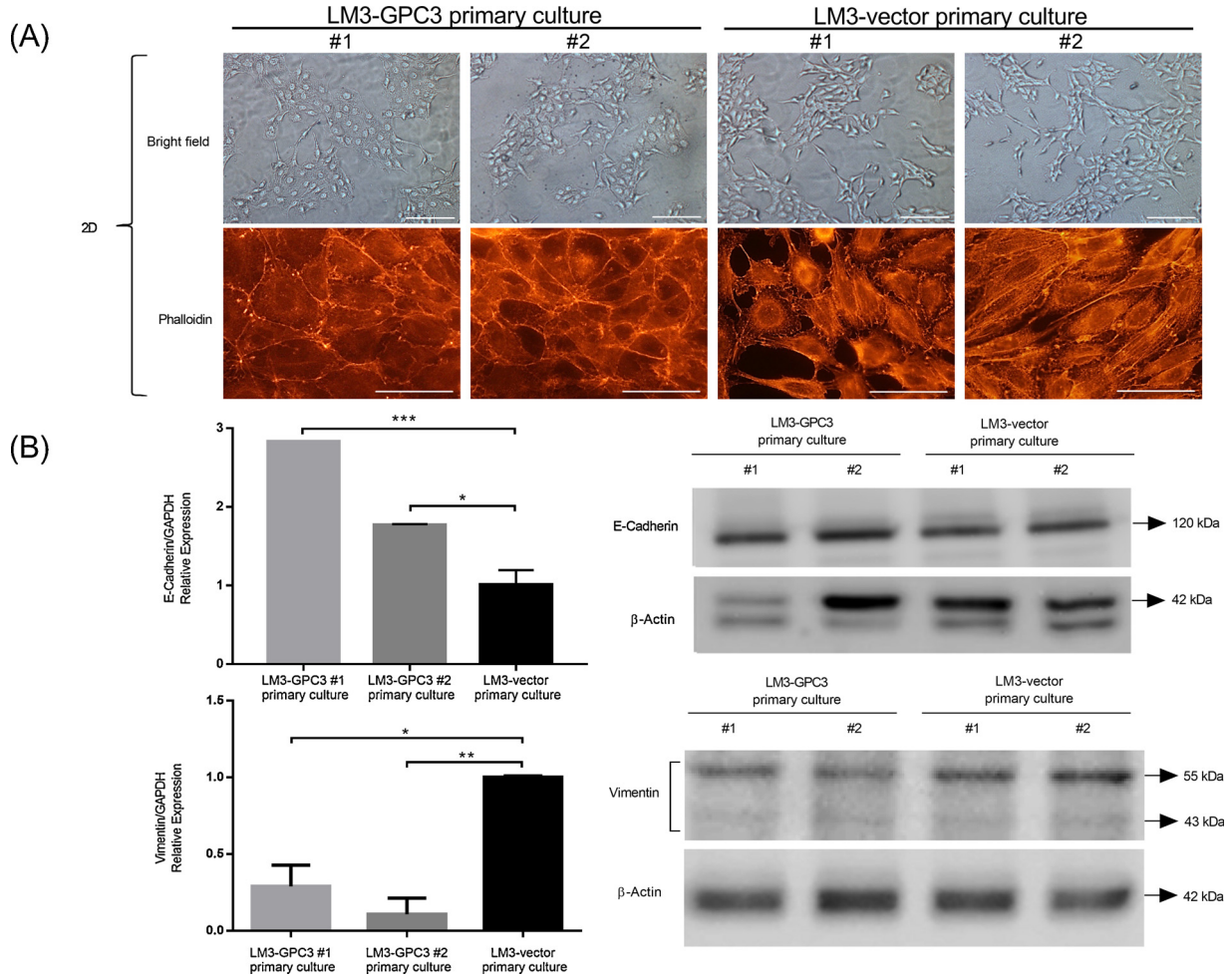

Fig. 4. Morphological features, actin cytoskeleton organization and EMT markers expression of "ex dormant" primary culture cells. Lungs from mice inoculated with GPC3 reexpressing cell sublines (without metastasis), and lungs from mice injected with control sublines (with macroscopic metastatic foci) were cultured and selected with G418 (n = 5 animals per group). The "ex dormant" primary culture cells were studied. (A) Morphological cell characteristics. *Top panel*: Cells were grown on coverslips and bright field (BF) images were taken (scale bars 100 μm). *Bottom panel*: To study the actin cytoskeleton, cells were stained with phalloidin-Alexa 546 and analyzed under fluorescence microscope (scale bars 50 μm). Images are representative of three independent experiments. (B) EMT markers expression. *Left panel:* E-Cadherin and Vimentin mRNA expression levels were identified by qPCR and GAPDH was used as control. Data is representative of three independent experiments. Bars represent mean values ± SD (*** $p < 0.001$, ** $p < 0.005$, * $p < 0.05$ ANOVA, Tukey´s multiple comparisons tests). *Right panel:* WB analysis was employed to determine E-Cadherin and Vimentin protein expression. β-Actin was used as an internal control. Numbers on the right represent molecular mass (kDa). Representative images of three independent experiments are shown.

demonstrated first that GPC3 leads the variations expected for putative dormant cells. In this sense, LM3-GPC3 clones exhibited a decreased phospho-Erk to phospho-p38 ratio and increased p21, p27 and SOX2 expression. Further, these findings translated to an inhibition of *in vivo* metastatic spread. Here it was established that GPC3 inhibits metastatic spread of mammary tumors through the induction of dormancy at the secondary site. Our data confirm that dormancy is a reversible state, given that when dormant cells are cultivated, they restart their growth. Importantly, "ex dormant cells" retained the properties of the parental line, including GPC3 and E-Cadherin expression. Our results are in association with features of a breast cancer metastasis suppressor 1 (BRMS-1) (Welch et al., 2016). Like GPC3, BRMS-1 has a key function

Table 1
LM3-GPC3 and LM3-vector primary culture cells *in vivo* behavior.

Tumor progression properties	LM3-GPC3 Primary culture		LM3-vector Primary culture	
	#1	#2	#1	#2
Tumorigenicity (%, n/n)	100 (5/5)	100 (5/5)	100 (5/5)	100 (5/5)
Tumor growth rate (cm^3/day)	0.100± 0.013	0.142± 0.006	0.063± 0.013	0.083± 0.038
Number of spontaneous pulmonary nodules (Md [Rg])	0 [0−8]**	0 [0−1]**	72.5 [35−170]	6 [1−57]
Spontaneous pulmonary nodules incidence (%, n/n)	40 (2/5)*	20 (1/5)*	100 (5/5)	100 (5/5)

Tumorigenicity: number of animals that developed tumors / number of injected animals. % percentage, n number.
Number of spontaneous pulmonary nodules: Md median; Rg range.
Spontaneous lung metastasis incidence: number of animals presenting distant metastasis / number of injected animals. % percentage, n number.
** $p < 0.005$ Kruskal-Wallis, Dunn´s test,* $p < 0.05$ chi-square test.

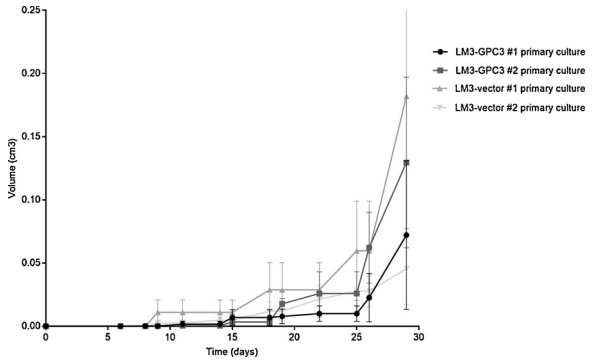

Fig. 5. *In vivo* subcutaneous tumor growth of "ex dormant" primary culture cells. 2-month old BALB/c virgin female mice (n = 5 animals per group) were subcutaneously inoculated with LM3-vector and LM3-GPC3 primary culture cells. Tumor volume, expressed in cm^3 as mean ± SD, was used as growth parameter. Similar results were obtained in another independent experiment (ns, Exponential growth equation).

in the ectopic tumor development, and induces metastatic dormancy (Phadke et al., 2008). Moreover, it was reported that an EMT blocking would participate too in the BRMS-1 metastasis suppressor function (Kodura and Souchelnytskyi, 2015).

It is important to note that in the present work we also confirmed that GPC3 reexpression does not affect the growth of subcutaneous tumors, as expected for metastasis suppressor. This is in association with data previously reported for parental sublines, both *in vivo* and *in vitro*. GPC3 did not modulate the *in vitro* proliferation rate of unsynchronized LM3 cell monolayers or the *in vivo* tumor growth ratio (Peters et al., 2003). The absence of a general growth inhibitory effect of GPC3 could indicate specificity for dormancy regulation at distant organ, as is suggested for metastasis suppressors. Here we provided experimental *in vivo* evidences demonstrating that LM3-GPC3 "ex dormant cells" are still viable and tumorigenic, but -like parental lines- they are not able to colonize secondary organs. In this work, by means of primary cultures of lungs without metastatic foci from LM3-GPC3 "ex dormant" tumors-bearing mice, we showed again the presence of dormant cells. In agreement, we previously reported a great inhibitory effect of GPC3 when LM3 cells were grown under highly restricted conditions, as the *in vitro* clonogenic assay is (Peters et al., 2003). The characteristics of this low density cell growth test could be interpreted like those that disseminated tumor cells (DTCs) are exposed after extravasation in secondary colonization site. In sum, this study is the first showing that although GPC3 reexpressing mammary tumor cells could complete all phases of the metastatic process, they do not colonize secondary sites. These GPC3 reexpressing cells persist in mouse lungs in a dormant state. We demonstrated that these cells can break dormancy and proliferate when they are cultured. LM3-GPC3 "ex dormant cells" cross total metastasis stages but they arrest at secondary site and re-enter in the non-dividing mode. Disseminated dormant tumor cells have widely been described in cancer patients (Rossari et al., 2019). These latent cells, besides to confer resistance to proliferation-dependent treatments like radiation and chemotherapy (Aguirre-Ghiso, 2006), are a risk for patients since they can abruptly breakout inactivity and develop lethal metastasis. Although it was suggested that the artificial reactivation of latent tumor cells would be usefulness for getting cells susceptible to conventional therapies (Bliss et al., 2014), this concept is dangerous since it could have side effects as well as induces relapse (Dittmer, 2017). Alternatively, it would be possible the development of therapies for promoting dormancy and thus preventing the re-work of DTCs. Here we describe the role of GPC3 in the dormant state induction, so it could be considered a key molecular target.

As we mentioned, it is key the identification of mechanisms regulating dormancy as well as the processes inducing dormancy escape. Here it was proven that GPC3 induces *in vivo* dormancy by p38 signaling activation. Our group previously described a relation between GPC3 and p38. We showed the activation of p38 signaling pathway (Buchanan et al., 2010) as well as we described the intricate system of reciprocity working among the pathways regulated by GPC3. Moreover, we recently showed that LM3-GPC3 cell sublines secret this glypican (Fernandez et al., 2018). Future studies are necessary to determine the membrane receptor with which secreted GPC3 interacts and, directly or indirectly, thus activates the p38 pathway.

Although the role of p38 in cellular dormancy was widely described (Aguirre-Ghiso et al., 2003; Kobayashi et al., 2011; Lenk et al., 2017; Yu-Lee et al., 2018), this is - to our knowledge- the first report associating GPC3, metastasis suppression and p38 MAPK activity. Through *in vivo* studies, employing animals treated with the pharmacological p38 inhibitor, we reliably showed that GPC3 needs an active p38 signaling to inhibit breast cancer metastatic spread. It is important to note that the inhibitor treatment did not affect subcutaneous tumor growth, but reversed metastatic development inhibition induced by GPC3. This data suggests that p38 would specifically control tumor growth at the secondary site. Even though this is the first work linking GPC3, p38 and dormancy, Adam et. al. demonstrated the association with other

Table 2
Effect of p38 MAPK signaling inhibition on LM3-GPC3 and LM3-vector cells *in vivo* behavior.

Tumor progression properties	LM3-GPC3				LM3-vector			
	SB203580		DMSO		SB203580		DMSO	
	#1	#2	#1	#2	#1	#2	#1	#2
Tumorigenicity (%, n/n)	100 (5/5)	100 (5/5)	100 (5/5)	100 (5/5)	100 (5/5)	100 (5/5)	100 (5/5)	100 (5/5)
Latency (days)(Md [Rg])	7 [7 – 8]	9 [8 – 12]	8 [7 – 23]	8 [6 – 10]	9 [7 – 10]	8 [8 – 9]	9.5 [9 – 10]	7.5 [7 – 9]
Tumor growth rate (cm^3/day)	0.019± 0.004	0.017± 0.009	0.016± 0.009	0.018± 0.002	0.014± 0.004	0.017± 0.003	0.011± 0.004	0.013± 0.003
Macroscopic invasion with ulceration (%, n/n)	100 (5/5)	80 (4/5)	20 (1/5) *	40 (2/5) *	100 (5/5)	100 (5/5)	100 (5/5)	80 (4/5)
Spontaneous lung metastases incidence (%, n/n)	80 (4/5)	80 (4/5)	0 (0/5) *	0 (0/5) *	100 (5/5)	100 (5/5)	100 (5/5)	100 (5/5)
Number of spontaneous pulmonary nodules (Md [Rg])	2 [0 – 5]	2 [0 – 6]	0 [0 – 0] &	0 [0 – 0] &	4 [1 – 10]	5 [2 – 18]	6 [3 – 24]	4 [1 – 19]
Number of experimental pulmonary nodules (Md [Rg])	20 [11 – 64]	35 [17 – 57]	11 [0 – 17] &	13 [2 – 19] &&	23 [15 – 67]	34 [15 – 70]	31 [10 – 52]	27 [22 – 30]

Tumorigenicity: number of animals that developed tumors / number of injected animals. % percentage, n number.
Latency: days for the first tumor palpation after injection. Md median; Rg range.
Macroscopic invasion with ulceration: number of animals with local invasion / total number of animals. % percentage, n number.
Spontaneous lung metastasis incidence: number of animals presenting distant metastasis / number of injected animals. % percentage, n number.
Number of spontaneous pulmonary nodules: Md median; Rg range.
Number of experimental pulmonary nodules: Md median; Rg range.
* $p < 0.05$ chi-square test; & $p < 0.05$; && $p < 0.005$ Kruskal-Wallis, Dunn´s tests.

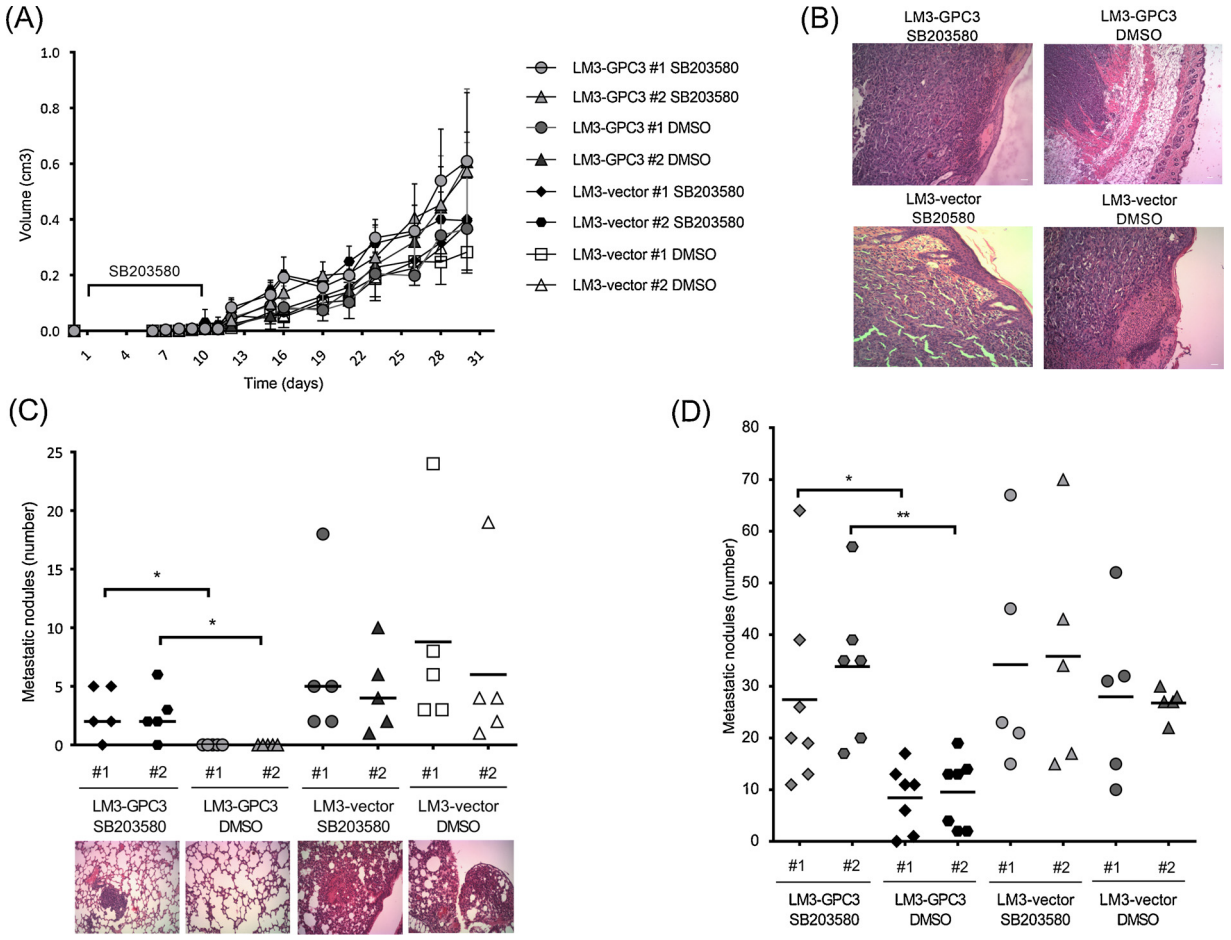

Fig. 6. Effects of p38 MAPK signaling pathway on *in vivo* behavior of GPC3 reexpressing breast cancer cell sublines. (A) LM3-GPC3 or LM3-vector cells were subcutaneously inoculated into BALB/c mice (n = 5 animals per group), and the p38 inhibitor SB203580 (or DMSO as control) was intraperitoneally administered. Tumor volume, expressed in cm^3 as mean ± SD, was used as growth parameter. Similar results were obtained in another independent experiment (ns, Exponential growth equation). (B) Subcutaneous tumors were histologically analyzed by hematoxylin-eosin staining. Representative photographs of two independent experiments are shown (scale bar 200 μm). (C) The lungs of tumor-bearing mice were removed and examined for spontaneous metastases under a dissecting microscope (* $p < 0.05$ Kruskal-Wallis, Dunn´s tests) and by histological staining. Representative images of two independent experiments are shown (Scale bar 200 μm). (D) LM3-GPC3 and LM3-vector sublines were intravenously inoculated into BALB/c mice (n = 5 animals per group) and the p38 inhibitor SB203580 (or DMSO as control) was administered. The number of metastatic lung foci was recorded 21 days post-inoculation. Data is representative of another independent experiment (* $p < 0.05$, ** $p < 0.005$ Kruskal-Wallis, Dunn´s test).

proteoglycan (Adam et al., 2009). The authors identified the molecular network regulated by p38, which is necessary for human squamous carcinoma cells quiescence. Interesting, among the 46 genes upregulated in dormant cells, there is GPC1 (another member of the glypican family) as well as several enzymes involved in glycan biosynthesis and degradation.

5. Conclusion

Here we corroborated that GPC3 reexpression returns mesenchymal-like breast cancer cells to an epithelial phenotype, induces dormancy and impairs *in vivo* metastatic spread. In addition, there were presented evidences about the mechanism by which GPC3 reprograms disseminated tumor cells to a dormant state by p38 MAPK signaling pathway activation. Our results help to detect cancer cell dormancy genetic contributing factors as well as suggest the usefulness of studies focusing GPC3, which could provide therapeutic approaches for preventing metastasis dissemination and cancer relapse.

Funding

This research was supported by funding from FONCyT (PICT 2013 - 1337) – Ministerio de Ciencia y Tecnica Argentina CONICET (PIP 2013 - 112200120100100CO) and Fundacion Florencio Fiorini, Argentina.

Declaration of Competing Interest

None. The authors declare that they have no known competing financial interests or personal relationships that could have appeared to influence the work reported in this paper.

Appendix A. Supplementary data

Supplementary material related to this article can be found, in the online version, at doi:https://doi.org/10.1016/j.ejcb.2020.151096.

References

Adam, A.P., George, A., Schewe, D., Bragado, P., Iglesias, B.V., Ranganathan, A.C., Kourtidis, A., Conklin, D.S., Aguirre-Ghiso, J.A., 2009. Computational identification of a p38SAPK-regulated transcription factor network required for tumor cell quiescence. Cancer Res. 69, 5664–5672.

Aguirre-Ghiso, J.A., 2006. The problem of cancer dormancy: understanding the basic mechanisms and identifying therapeutic opportunities. Cell Cycle 5, 1740–1743.

Aguirre-Ghiso, J.A., Estrada, Y., Liu, D., Ossowski, L., 2003. ERK(MAPK) activity as a determinant of tumor growth and dormancy; regulation by p38(SAPK). Cancer Res.

63, 1684–1695.
Bliss, S.A., Greco, S.J., Rameshwar, P., 2014. Hierarchy of breast cancer cells: key to reverse dormancy for therapeutic intervention. Stem Cells Transl. Med. 3, 782–786.
Bragado, P., Estrada, Y., Parikh, F., Krause, S., Capobianco, C., Farina, H.G., Schewe, D.M., Aguirre-Ghiso, J.A., 2013. TGF-beta2 dictates disseminated tumour cell fate in target organs through TGF-beta-RIII and p38alpha/beta signalling. Nat. Cell Biol. 15, 1351–1361.
Buchanan, C., Stigliano, I., Garay-Malpartida, H.M., Rodrigues Gomes, L., Puricelli, L., Sogayar, M.C., Bal de Kier Joffe, E., Peters, M.G., 2010. Glypican-3 reexpression regulates apoptosis in murine adenocarcinoma mammary cells modulating PI3K/Akt and p38MAPK signaling pathways. Breast Cancer Res. Treat. 119, 559–574.
Buchanan, C., Lago Huvelle, M.A., Peters, M.G., 2011. Metastasis suppressors: basic and translational advances. Curr. Pharm. Biotechnol. 12, 1948–1960.
Capurro, M., Wanless, I.R., Sherman, M., Deboer, G., Shi, W., Miyoshi, E., Filmus, J., 2003. Glypican-3: a novel serum and histochemical marker for hepatocellular carcinoma. Gastroenterology 125, 89–97.
Capurro, M.I., Xiang, Y.Y., Lobe, C., Filmus, J., 2005. Glypican-3 promotes the growth of hepatocellular carcinoma by stimulating canonical Wnt signaling. Cancer Res. 65, 6245–6254.
Castillo, L., Lago Huvelle, M.A., Fujita, A., Ramos Lobba Maia, A., Tascón, R., Romera Garcia, T., Armanasco, E., Bagnoli, F., Marques de Oliveira, V., Longo Galvao, M.A., Montor, W., Sogayar, M., Bal de Kier Joffé, E., Puricelli, L., Labriola, L., Peters, M.G., 2015. Expression of Glypican-3 (GPC3) in malignant and non-malignant human breast tissues. Open Cancer J. 8, 12–23.
Castillo, L.F., Tascon, R., Huvelle, M.A., Novack, G., Llorens, M.C., Santos, A.F., Shortrede, J., Cabanillas, A.M., Joffe, E.B., Labriola, L., Peters, M.G., 2016. Glypican-3 induces a mesenchymal to epithelial transition in human breast cancer cells. Oncotarget.
Chui, M.H., Have, C., Hoang, L.N., Shaw, P., Lee, C.H., Clarke, B.A., 2018. Genomic profiling identifies GPC5 amplification in association with sarcomatous transformation in a subset of uterine carcinosarcomas. J. Pathol. Clin. Res. 4, 69–78.
De Craene, B., Berx, G., 2013. Regulatory networks defining EMT during cancer initiation and progression. Nat. Rev. Cancer 13, 97–110.
Dittmer, J., 2017. Mechanisms governing metastatic dormancy in breast cancer. Semin. Cancer Biol. 44, 72–82.
Djomehri, S.I., Burman, B., Gonzalez, M.E., Takayama, S., Kleer, C.G., 2019. A reproducible scaffold-free 3D organoid model to study neoplastic progression in breast cancer. J. Cell Commun. Signal. 13, 129–143.
Fernandez, D., Guereno, M., Lago Huvelle, M.A., Cercato, M., Peters, M.G., 2018. Signaling network involved in the GPC3-induced inhibition of breast cancer progression: role of canonical Wnt pathway. J. Cancer Res. Clin. Oncol. 144, 2399–2418.
Filmus, J., 2001. Glypicans in growth control and cancer. Glycobiology 11, 19R–23R.
Filmus, J., Selleck, S.B., 2001. Glypicans: proteoglycans with a surprise. J. Clin. Invest. 108, 497–501.
Filmus, J., Shi, W., Wong, Z.M., Wong, M.J., 1995. Identification of a new membrane-bound heparan sulphate proteoglycan. Biochem. J. 311 (Pt 2), 561–565.
Filmus, J., Capurro, M., Rast, J., 2008. Glypicans. Genome Biol. 9, 224.
Gao, W., Kim, H., Ho, M., 2015. Human monoclonal antibody targeting the heparan sulfate chains of Glypican-3 inhibits HGF-Mediated migration and motility of hepatocellular carcinoma cells. PLoS One 10, e0137664.
Gonzalez, D.M., Medici, D., 2014. Signaling mechanisms of the epithelial-mesenchymal transition. Sci. Signal. 7 re8.
Han, S., Ma, X., Zhao, Y., Zhao, H., Batista, A., Zhou, S., Zhou, X., Yang, Y., Wang, T., Bi, J., Xia, Z., Bai, Z., Garkavtsev, I., Zhang, Z., 2016. Identification of Glypican-3 as a potential metastasis suppressor gene in gastric cancer. Oncotarget 7, 44406–44416.
Horak, C.E., Lee, J.H., Marshall, J.C., Shreeve, S.M., Steeg, P.S., 2008. The role of metastasis suppressor genes in metastatic dormancy. APMIS 116, 586–601.
Iglesias, B.V., Centeno, G., Pascuccelli, H., Ward, F., Peters, M.G., Filmus, J., Puricelli, L., de Kier Joffe, E.B., 2008. Expression pattern of glypican-3 (GPC3) during human embryonic and fetal development. Histol. Histopathol. 23, 1333–1340.
Kim, H., Xu, G.L., Borczuk, A.C., Busch, S., Filmus, J., Capurro, M., Brody, J.S., Lange, J., D'Armiento, J.M., Rothman, P.B., Powell, C.A., 2003. The heparan sulfate proteoglycan GPC3 is a potential lung tumor suppressor. Am. J. Respir. Cell Mol. Biol. 29, 694–701.
Kobayashi, A., Okuda, H., Xing, F., Pandey, P.R., Watabe, M., Hirota, S., Pai, S.K., Liu, W., Fukuda, K., Chambers, C., Wilber, A., Watabe, K., 2011. Bone morphogenetic protein 7 in dormancy and metastasis of prostate cancer stem-like cells in bone. J. Exp. Med. 208, 2641–2655.
Kodura, M.A., Souchelnytskyi, S., 2015. Breast carcinoma metastasis suppressor gene 1 (BRMS1): update on its role as the suppressor of cancer metastases. Cancer Metastasis Rev. 34, 611–618.
Kumar, S., Jiang, M.S., Adams, J.L., Lee, J.C., 1999. Pyridinylimidazole compound SB 203580 inhibits the activity but not the activation of p38 mitogen-activated protein kinase. Biochem. Biophys. Res. Commun. 263, 825–831.
Lenk, L., Pein, M., Will, O., Gomez, B., Viol, F., Hauser, C., Egberts, J.H., Gundlach, J.P., Helm, O., Tiwari, S., Weiskirchen, R., Rose-John, S., Rocken, C., Mikulits, W., Wenzel, P., Schneider, G., Saur, D., Schafer, H., Sebens, S., 2017. The hepatic microenvironment essentially determines tumor cell dormancy and metastatic outgrowth of pancreatic ductal adenocarcinoma. Oncoimmunology 7, e1368603.
Lin, H., Huber, R., Schlessinger, D., Morin, P.J., 1999. Frequent silencing of the GPC3 gene in ovarian cancer cell lines. Cancer Res. 59, 807–810.
Lorusso, G., Ruegg, C., 2012. New insights into the mechanisms of organ-specific breast cancer metastasis. Semin. Cancer Biol. 22, 226–233.
Mizushima, S., Nagata, S., 1990. pEF-BOS, a powerful mammalian expression vector. Nucleic Acids Res. 18, 5322.
Murthy, S.S., Shen, T., De Rienzo, A., Lee, W.C., Ferriola, P.C., Jhanwar, S.C., Mossman, B.T., Filmus, J., Testa, J.R., 2000. Expression of GPC3, an X-linked recessive overgrowth gene, is silenced in malignant mesothelioma. Oncogene 19, 410–416.
Nash, K.T., Phadke, P.A., Navenot, J.M., Hurst, D.R., Accavitti-Loper, M.A., Sztul, E., Vaidya, K.S., Frost, A.R., Kappes, J.C., Peiper, S.C., Welch, D.R., 2007. Requirement of KISS1 secretion for multiple organ metastasis suppression and maintenance of tumor dormancy. J. Natl. Cancer Inst. 99, 309–321.
Norkin, M., Uberti, J.P., Schiffer, C.A., 2011. Very late recurrences of leukemia: why does leukemia awake after many years of dormancy? Leuk. Res. 35, 139–144.
Pellegrini, M., Pilia, G., Pantano, S., Lucchini, F., Uda, M., Fumi, M., Cao, A., Schlessinger, D., Forabosco, A., 1998. Gpc3 expression correlates with the phenotype of the Simpson-Golabi-Behmel syndrome. Dev. Dyn. 213, 431–439.
Peters, M.G., Farias, E., Colombo, L., Filmus, J., Puricelli, L., Bal de Kier Joffe, E., 2003. Inhibition of invasion and metastasis by glypican-3 in a syngeneic breast cancer model. Breast Cancer Res. Treat. 80, 221–232.
Phadke, P.A., Vaidya, K.S., Nash, K.T., Hurst, D.R., Welch, D.R., 2008. BRMS1 suppresses breast cancer experimental metastasis to multiple organs by inhibiting several steps of the metastatic process. Am. J. Pathol. 172, 809–817.
Rossari, F., Zucchinetti, C., Buda, G., Orciuolo, E., 2019. Tumor dormancy as an alternative step in the development of chemoresistance and metastasis - clinical implications. Cell. Oncol. Dordr. (Dordr).
Sosa, M.S., Parikh, F., Maia, A.G., Estrada, Y., Bosch, A., Bragado, P., Ekpin, E., George, A., Zheng, Y., Lam, H.M., Morrissey, C., Chung, C.Y., Farias, E.F., Bernstein, E., Aguirre-Ghiso, J.A., 2015. NR2F1 controls tumour cell dormancy via SOX9- and RARbeta-driven quiescence programmes. Nat. Commun. 6, 6170.
Stigliano, I., Puricelli, L., Filmus, J., Sogayar, M.C., Bal de Kier Joffe, E., Peters, M.G., 2009. Glypican-3 regulates migration, adhesion and actin cytoskeleton organization in mammary tumor cells through Wnt signaling modulation. Breast Cancer Res. Treat. 114, 251–262.
Sugimura, J., Foster, R.S., Cummings, O.W., Kort, E.J., Takahashi, M., Lavery, T.T., Furge, K.A., Einhorn, L.H., Teh, B.T., 2004. Gene expression profiling of early- and late-relapse nonseminomatous germ cell tumor and primitive neuroectodermal tumor of the testis. Clin. Cancer Res. 10, 2368–2378.
Sun, Y., Xu, K., He, M., Fan, G., Lu, H., 2018. Overexpression of Glypican 5 (GPC5) Inhibits Prostate Cancer Cell Proliferation and Invasion via Suppressing Sp1-Mediated EMT and Activation of Wnt/beta-Catenin Signaling. Oncol. Res. 26, 565–572.
Toretsky, J.A., Zitomersky, N.L., Eskenazi, A.E., Voigt, R.W., Strauch, E.D., Sun, C.C., Huber, R., Meltzer, S.J., Schlessinger, D., 2001. Glypican-3 expression in Wilms tumor and hepatoblastoma. J. Pediatr. Hematol. Oncol. 23, 496–499.
Torre, L.A., Islami, F., Siegel, R.L., Ward, E.M., Jemal, A., 2017. Global Cancer in women: burden and trends. Cancer Epidemiol. Biomarkers Prev. 26, 444–457.
Urtreger, A., Ladeda, V., Puricelli, L., Rivelli, A., Vidal, M.C., Lustig, E.S., Bal de Kier Joffé, E., 1997. Modulation of fibronectin expression and proteolytic activity associated with the invasive and metastatic phenotype in two murine mammary cell lines. Int. J. Oncol. 11, 489–496.
Valsechi, M.C., Oliveira, A.B., Conceicao, A.L., Stuqui, B., Candido, N.M., Provazzi, P.J., de Araujo, L.F., Silva Jr., W.A., Calmon Mde, F., Rahal, P., 2014. GPC3 reduces cell proliferation in renal carcinoma cell lines. BMC Cancer 14, 631.
Wang, S., Qiu, M., Xia, W., Xu, Y., Mao, Q., Wang, J., Dong, G., Xu, L., Yang, X., Yin, R., 2016. Glypican-5 suppresses Epithelial-Mesenchymal Transition of the lung adenocarcinoma by competitively binding to Wnt3a. Oncotarget 7, 79736–79746.
Welch, D.R., Manton, C.A., Hurst, D.R., 2016. Breast Cancer metastasis suppressor 1 (BRMS1): robust biological and pathological data, but still enigmatic mechanism of action. Adv. Cancer Res. 132, 111–137.
Wu, Y., Liu, H., Weng, H., Zhang, X., Li, P., Fan, C.L., Li, B., Dong, P.L., Li, L., Dooley, S., Ding, H.G., 2015. Glypican-3 promotes epithelial-mesenchymal transition of hepatocellular carcinoma cells through ERK signaling pathway. Int. J. Oncol. 46, 1275–1285.
Yu-Lee, L.Y., Yu, G., Lee, Y.C., Lin, S.C., Pan, J., Pan, T., Yu, K.J., Liu, B., Creighton, C.J., Rodriguez-Canales, J., Villalobos, P.A., Wistuba II., de, Nadal, E., Posas, F., Gallick, G.E., Lin, S.H., 2018. Osteoblast-secreted factors mediate dormancy of metastatic prostate Cancer in the bone via activation of the TGFbetaRIII-p38MAPK-pS249/T252RB pathway. Cancer Res. 78, 2911–2924.
Zittermann, S.I., Capurro, M.I., Shi, W., Filmus, J., Soluble glypican 3 inhibits the growth of hepatocellular carcinoma in vitro and in vivo. International journal of cancer. Journal international du cancer 126, 1291-1301.